JPET Fast Forward. Published on October 2, 2006 as DOI: 10.1124/jpet.106.110411

JPET #110411

Title Page

4-aminopyridine prevents the conformational changes associated with P/C-type inactivation in *Shaker* channels

Thomas W Claydon, Moni Vaid, Saman Rezazadeh, Steven J. Kehl and David Fedida

Departments of Anesthesiology, Pharmacology & Therapeutics (TWC, DF) and Cellular and Physiological Sciences (MV, SR, SJK)
University of British Columbia
Vancouver, British Columbia
V6T 1Z3, Canada

Running Title Page

Running title: Inactivation and 4-AP binding

Correspondence to: Dr. David Fedida,
Department of Anesthesiology, Pharmacology & Therapeutics and Cellular and Physiological Sciences
2350 Health Sciences Mall, Vancouver B.C. V6T 1Z3
Canada
Tel: (604) 822-5806; FAX: (604) 822-2316;
E-mail: fedida@interchange.ubc.ca

Number of text pages: 37
Number of Tables: 0
Number of Figures: 6
Number of References: 41
Number of Words in Abstract: 250
Number of Words in Introduction: 781
Number of Words in Discussion: 1320
Recommended Section Assignment: Neuropharmacology

List of Abbreviations: 4-AP, 4-aminopyridine; G, chord conductance; IC_{50}, the concentration required to achieve half maximal block; *k*, slope factor; Kv, voltage-gated potassium channels; $V_{1/2}$, half-activation potential; TMRM, tetramethylrhodamine-5-maleimide.

Abstract:

The effect of 4-AP on Kv channel activation has been extensively investigated, but its interaction with inactivation is less well understood. Voltage clamp fluorimetry was used to directly monitor the action of 4-AP on conformational changes associated with slow inactivation of *Shaker* channels. Tetramethylrhodamine-5-maleimide was used to fluorescently label substituted cysteine residues in the S3-S4 linker (A359C) and pore (S424C). Activation- and inactivation-induced changes in fluorophore microenvironment produced fast and slow phases of fluorescence that were modified by 4-AP. In *Shaker* A359C, 4-AP block reduced the slow phase contribution from 61 ± 3 to 28 ± 5% suggesting that binding inhibits the conformational changes associated with slow inactivation, and increased the fast phase that reports channel activation from 39 ± 3 to 72 ± 5%. In addition, 4-AP enhanced both fast and slow phases of fluorescence return upon repolarization (τ reduced from 87 ± 15 to 40 ± 1 ms and from 739 ± 83 to 291 ± 21 ms, respectively) suggesting that deactivation and recovery from inactivation were enhanced. Also, the effect of 4-AP on the slow phase of fluorescence was dramatically reduced in channels with either reduced (T449V) or permanent P-type (W434F) inactivation. Interestingly, the slow phase of fluorescence return of W434F channels was enhanced by 4-AP suggesting that 4-AP prevents the transition to C-type inactivation in these channels. These data directly demonstrate that 4-AP prevents slow inactivation of Kv channels and that 4-AP can bind to P-type inactivated channels and selectively inhibit the onset of C-type inactivation.

JPET Fast Forward. Published on October 2, 2006 as DOI: 10.1124/jpet.106.110411
This article has not been copyedited and formatted. The final version may differ from this version.

Introduction:

4-aminopyridine (4-AP) is a voltage-gated K^+ (Kv) channel blocker that is useful clinically in the treatment of spinal cord injuries (Wolfe et al., 2001), and multiple sclerosis (Bever, Jr. et al., 1996). In addition to its therapeutic applications, 4-AP is routinely used to isolate different types of Kv channels expressed in native tissues based on their affinities for the drug (Grissmer et al., 1994; Shieh and Kirsch, 1994), and also to study the biophysical properties of cloned Kv channels (Kirsch and Drewe, 1993; Shieh et al., 1997; del Camino et al., 2005). It is well accepted that 4-AP is an intracellular blocker of Kv channels (Kirsch and Narahashi, 1983; Kirsch and Drewe, 1993; Choquet and Korn, 1992; Bouchard and Fedida, 1995; Tseng et al., 1996; see also Fig. 1A), but the mechanism of 4-AP block is complex and the pathways that have been proposed have involved preferential binding to closed (Kirsch and Narahashi, 1983; Kirsch et al., 1986), open (Choquet and Korn, 1992; McCormack et al., 1994; Castle et al., 1994; Yao and Tseng, 1994; Bouchard and Fedida, 1995), and inactivated states of the channel (Thompson, 1982). It is documented that 4-AP cannot access its binding site when the channel is closed (with the exception of Kv4.2 channels where 4-AP binding occurs exclusively in the closed state (Kehl, 1990; Tseng, et al., 1996)), because channels only show block and unblock after membrane depolarization to potentials that induce significant channel opening (Choquet and Korn, 1992; McCormack et al., 1994; Castle et al., 1994; Bouchard and Fedida, 1995; see also Fig. 1B). Furthermore, the recovery of ionic currents after 4-AP washout is contingent on channel opening, which suggests that 4-AP becomes trapped in closed channels and prevents their re-opening (Choquet and Korn, 1992; Kirsch and Drewe, 1993; Bouchard and Fedida, 1995; del Camino et al., 2005). A working model of 4-AP binding (Armstrong and Loboda,

2001) suggests that the drug displaces the hydrated K^+ that is trapped in the intracellular cavity (Ray and Deutsch, 2006), causing closure of intracellular activation gate.

In support of this idea, 4-AP causes very subtle changes in channel on-gating currents (Loboda and Armstrong, 2001), but very profound changes in off-gating (McCormack et al., 1994; Bouchard and Fedida, 1995; Loboda and Armstrong, 2001). Specifically, 4-AP prevents the slowing of charge return that occurs on repolarization from potentials that cause channel opening, which suggests that 4-AP selectively blocks the concerted opening step in the activation sequence without altering the early independent gating transitions (Armstrong and Loboda, 2001; Pathak et al., 2005; del Camino et al., 2005). Further support for this mechanism of action comes from experiments using the *Shaker* ILT mutation (Pathak et al., 2005), which energetically dissociates the early independent gating transitions from the last concerted opening transition (Smith-Maxwell et al., 1998a, b). Fig. 1B shows a gating scheme (simplified from that of Armstrong and Loboda (2001)) that summarizes these actions of 4-AP on activation gating.

Although the disruption of channel activation by 4-AP has been extensively investigated, as described above, the relationship between 4-AP block and channel inactivation is less well understood. Castle and co-workers (1994) used complex voltage clamp protocols to demonstrate that inactivation and 4-AP binding to *Shaker* and Kv1.1 channels were mutually exclusive, but since then, few additional studies have been performed. The recent development of site-directed voltage clamp fluorimetry allows the real-time monitoring of conformational changes associated with channel gating that do not result in ionic current (Mannuzzu et al., 1996; Cha and Bezanilla, 1997). This is accomplished by examining the changes in the emission from fluorescently-labeled residues, brought about by modifications of the fluorophore microenvironment as the channels activate and inactivate (Loots and Isacoff, 1998; Bezanilla, 2002). By attaching

TMRM at A359C in the S3-S4 linker and at S424C in the outer pore (Fig. 1A), the conformational rearrangements associated with movement of the voltage sensor during channel activation and of the pore during inactivation can be directly observed. For example, fluorescence changes from TMRM attached at A359C occur with the same voltage dependence as movement of the voltage sensor charge (Mannuzzu et al, 1996; Cha and Bezanilla, 1997), and the slow fluorescence deflection from TMRM attached at S424C occurs on a similar timescale to slow inactivation and is sensitive to manipulations that alter its rate (Loots and Isacoff, 1998). Here, we have used this technique to scrutinize directly the effect of 4-AP on slow inactivation of *Shaker* channels. Relevant amino acid sites used in this study are shown in Fig. 1A. We show that 4-AP prevents the conformational changes in *Shaker* channels associated with inactivation. Furthermore, we show that 4-AP can bind to P-type inactivated channels and inhibit the onset of C-type inactivation.

Materials and Methods:

Solutions and chemicals:

Barth's medium contained (in mM) 88 NaCl, 1 KCl, 2.4 $NaHCO_3$, 0.82 $MgSO_4$, 0.33 $Ca(NO_3)_2$, 0.41 $CaCl_2$, 20 HEPES, titrated to pH 7.4 using NaOH. ND96 bath solution contained (in mM): 96 NaCl, 3 KCl, 1 $MgCl_2$, 2 $CaCl_2$, and 5 HEPES, titrated to pH 7.4 using NaOH. TMRM labeling of oocytes was performed in a depolarizing solution that contained (in mM): 98 KCl, 1 $MgCl_2$, 2 $CaCl_2$ and 5 HEPES, titrated to pH 7.4 using KOH, and 50 μM TMRM. Working concentrations of 4-AP were diluted from a 100 mM stock solution made with ND96 solution and titrated to pH 7.4 using NaOH. All chemicals were purchased from Sigma-Aldrich (Mississauga, Ontario).

Molecular biology and RNA preparation:

A modified pBluescript SKII oocyte expression vector (pEXO) was used to express the N-terminal deletion mutant *Shaker* Δ6-46 (a kind gift from Dr. A. Sivaprasadarao) that is fast inactivation removed (Hoshi et al., 1991) and the pBluescript SKII expression vector was used to express *Shaker* Δ6-46 ILT (a kind gift from Dr. E. Isacoff).

The A359C and S424C mutations were made in the background of a mutation that replaced the only externally accessible cysteine residue, found in the S1-S2 linker, with a valine residue (C245V). This was done to reduce non-specific labeling and to introduce a cysteine residue for site-specific labeling with TMRM in either the S3-S4 linker (A359C) or the outer pore (turret) region (S424C). We use the terms *Shaker* A359C and *Shaker* S424C to describe the *Shaker* Δ6-46 C245V A359C and *Shaker* Δ6-46 C245V S424C mutant channels, respectively, throughout the manuscript. The T449V mutation in *Shaker* was used to inhibit slow inactivation

(Lopez-Barneo et al., 1993) and the W434F mutation was used to permanently inactivate channels (Perozo et al., 1993; Yang et al., 1997). Point mutations were generated using the Stratagene Quikchange kit (Stratagene, La Jolla, CA). All primers used were synthesized by Sigma Genosys (Oakville, Ontario). All constructs were sequenced using the core facility unit at the University of British Columbia. cDNA was linearized using BstEII (for *Shaker* Δ6-46 channels) or HindIII (for *Shaker* Δ6-46 ILT channels). cRNA was synthesized from linear cDNA using the T7 mMessage mMachine T7 Ultra cRNA transcription kit (Ambion, Austin, TX).

Oocyte preparation and Injection:

Xenopus laevis oocytes were prepared and isolated as described previously (Claydon et al., 2000). Briefly, gravid frogs were terminally anesthetized and stage V-VI oocytes were isolated and defolliculated using a combination of collagenase treatment (1 h in 1 mg/ml collagenase type 1; Sigma-Aldrich) and manual defolliculation. Oocytes were injected with 50 nl (5-10 ng) cRNA using a Drummond digital microdispenser (Fisher Scientific, Ontario, Canada) and then incubated in Barth's medium at 19 °C. Currents were recorded 1-7 days after injection.

Voltage-clamp fluorimetry:

Labeling of introduced cysteine residues was performed with tetramethylrhodamine-5-maleimide (TMRM, Invitrogen), which reacts specifically with cysteine residues and has a maximum light absorption at 542 nm and a maximum emission at 567 nm. Oocytes were washed and labeled with 50 μM TMRM in oocyte depolarizing solution for 30 min at 10 °C in

the dark. Oocytes were then placed in ND96 solution in the dark until being voltage clamped at room temperature. Fluorimetry was performed using a Nikon TE300 inverted microscope with Epi-Fluorescence attachment and a 9412b Electron Tubes photomultiplier tube (PMT) module (Cairn Research, Kent, UK). The TMRM dye was excited by light from a 100 W mercury lamp that was filtered with a 525 nm band pass excitation filter and passed via a dichroic mirror and 20x objective to the oocyte in the bath chamber. Fluorescence emission from the dye was collected via the same 20x objective and filtered through a 565 nm long pass emission filter before being passed to the PMT recording module. Voltage signals from the PMT were then digitized using an Axon Digidata 1322 A/D converter and passed to a computer running pClamp8 software (Axon Instruments, Foster City, CA) to record the fluorescence emission intensity. Fluorescence signals were filtered at 1 kHz with a sampling frequency of 20 kHz (when the pulse duration was 100 ms), 10 kHz (when the pulse duration was 7 s) or 2 kHz (when the pulse duration was 42 s). Traces were not averaged, except for those recorded during 100 ms pulses, which represent the average of five sweeps. To account for the majority of bleaching of the fluorescence signal during 7 or 42 s pulses, the fluorescence recorded during a pulse to -80 mV, where there is no voltage-dependent deflection, was subtracted. Simultaneous voltage clamp of the oocyte and acquisition of the current and voltage signals was achieved using the two-microelectrode voltage clamp technique with a Warner Instruments OC-725C amplifier (Hamden, CT), Axon Digidata 1322 and pClamp8 software. Microelectrodes were filled with 3 M KCl and had a resistance of 0.5-1.5 MΩ.

Data analysis:

JPET Fast Forward. Published on October 2, 2006 as DOI: 10.1124/jpet.106.110411
This article has not been copyedited and formatted. The final version may differ from this version.

G-V curves throughout the text were derived using the normalized chord conductance, which was calculated by dividing the maximum current during a depolarizing step by the driving force derived from the K^+ equilibrium potential (internal $[K^+]$ was assumed to be 98 mM). *G-V* curves were fitted with a single Boltzmann function:

$$y = 1/1(1 + \exp(V_{1/2} - V)/k)) \quad (1)$$

where y is the conductance normalized with respect to the maximal conductance, $V_{1/2}$ is the half-activation potential, V is the test voltage and k is the slope factor.

The Hill equation was used to fit the concentration-response relationship of the effect of 4-AP using GraphPad Prism 3.02 (San Diego, CA):

$$y=1/(1+(IC_{50}/[4\text{-AP}])^n) \quad (2)$$

where y is the fraction of current remaining at a given membrane potential, IC_{50} is the concentration required to achieve half maximal block, [4-AP] is the concentration of 4-AP in the bath solution, and n is the Hill coefficient. Data throughout the text and figures are shown as means ± S.E.M.

Results:

Shaker A359C TMRM fluorescence can report both channel activation and inactivation

The slow decay of Kv channel current during prolonged depolarizations involves at least two consecutive steps (see Yellen, 1998 and Kurata and Fedida, 2006), with the first step closing the outer pore (P-type inactivation) and allowing subsequent stabilization of the inactivated state (C-type inactivation), which is reported by stabilization of the activated conformation of the voltage sensor (DeBiasi et al., 1993; Olcese et al., 1997; Yang et al., 1997; Loots and Isacoff, 1998, 2000; see also Fig. 1B). Although these processes were first described using standard voltage clamp techniques, changes of channel conformation during P- and C-type inactivation can also be clearly observed using voltage clamp fluorimetry (Loots and Isacoff, 1998, 2000). In particular, two sites effectively report the conformational changes occurring during slow inactivation, A359 in the S3-S4 linker, and S424 in the pore. Data in Fig. 2A show typical current and fluorescence recordings from *Shaker* A359C channels (Figs. 2A and B), and two *Shaker* mutants with disrupted inactivation, T449V (Figs. 2D and E) and W434F (Figs. 2G and H). Currents are recorded during 100 ms pulses to a range of potentials that activate ionic current; the currents activate rapidly, and at the more positive potentials, decay (inactivate) during the sustained clamp pulse. On the time base studied here, the extent of the decay is small, but clearly seen in comparison to the horizontal dotted line that shows a single exponential fit of the rising phase of current. Fluorescence recordings (Fig. 2B) obtained simultaneously with the currents in panel A show a similar rapid onset, here manifested as a decrease in fluorescence, followed at the more positive clamp potentials by a slower declining phase, which corresponds to the current decay seen in Fig. 2A. It has been suggested that the rapid fluorescence decrease reported by A359C represents channel activation, while the slower decay phase reflects channel

JPET Fast Forward. Published on October 2, 2006 as DOI: 10.1124/jpet.106.110411
This article has not been copyedited and formatted. The final version may differ from this version.

inactivation (Loots and Isacoff, 1998). The amplitudes of the fast (F_{fast}) and slow (F_{slow}) phases of the fluorescence report from Fig. 2B are plotted together with the activating and inactivating components of the ionic current record, as a function of the potential during the clamp step in Fig. 2C. It can be seen that the rapid phase of fluorescence change, F_{fast}, is negatively shifted from the conductance-voltage relation (*G-V*) on the voltage axis as it reports the voltage sensor movement that precedes channel opening (Mannuzzu et al., 1996; Cha and Bezanilla, 1997). In *Shaker* A359C channels, F_{fast} contributes 64 ± 7 % to the total fluorescence deflection during a 100 ms pulse to +100 mV (n=10). The voltage-dependence of the slow phase of fluorescence deflection, F_{slow}, is displaced to the right of the fast fluorescence relationship, and shows a voltage-dependence similar to that for the *G-V* relation and also the inactivating component of current (I_{inact}), which is a plot of the amplitude of the current that decays during the pulse at each test potential (I_{inact} at each potential is normalized to that at +100 mV). This is expected since inactivation is coupled to channel opening and should approximate the *G-V* relation. F_{slow} contributes 36 ± 7 % to the total fluorescence deflection (n=10). The idea that the slow phase of fluorescence deflection is associated with channel inactivation is supported by experiments on two mutant channels with altered properties of slow inactivation (Fig. 2D-2I).

The mutation T449V in the outer mouth of the *Shaker* channel pore has long been used to disrupt slow inactivation (Lopez-Barneo et al., 1993). Current records in Fig. 2D and the voltage relations in Fig. 2F show that, as expected, the slow phase of current decay attributable to slow inactivation is largely prevented in this channel (i.e., I_{inact} is absent on this timescale). Consistent with this, the slow phase of fluorescence decay recorded from A359C is also absent (Fig. 2E, 2F). A second mutation, W434F, is known to induce permanent P-type inactivation (Perozo et al., 1993; Yang et al., 1997; Olcese et al., 1997; Loots and Isacoff, 1998), and there are no ionic

currents recordable from this mutant (Fig. 2G), but the fluorescence report is still robust (Fig. 2H), as activation proceeds normally despite the channels being inactivated (Perozo et al., 1993; Olcese et al., 1997; Starkus et al., 1998). It can be seen that although the fast phase of fluorescence is preserved, the slow fluorescence changes are completely abolished (Fig. 2H and 2I). Taken together, the results in Fig. 1 clearly demonstrate that the fluorescence report from A359C can track conformational changes associated with *Shaker* channel activation and of particular importance for the purposes of this study, channel inactivation. Even though channels may be unable to conduct, either before opening, or after inactivation, the fluorophore remains able to report changes in channel gating state.

The effect of 4-AP on channel inactivation

Using voltage-clamp fluorimetry, we investigated the effect of 4-AP on the conformational rearrangements associated with channel inactivation by recording ionic currents and fluorescence signals from TMRM attached at A359C during 7 s depolarizing pulses to +60 mV in the absence and presence of 3 mM 4-AP (Fig. 3A). In the control trace, channels open rapidly upon depolarization, but then during maintained depolarization the current declines due to the onset of slow (P- then C-type) inactivation. The signal from the fluorophore in the S3-S4 linker (Fig. 3A, lower panel) reports on the conformational changes associated with these gating events. On depolarization, there is a rapid fluorescence deflection followed by a slowly declining phase, which displays kinetics similar to the decay of ionic current and represents the transition of channels into the inactivated conformation as described in Fig. 2. This is highlighted in Fig. 3B, which shows superimposed traces of ionic current and fluorescence signal decay recorded simultaneously from the same cell. The mean time constants of decay for the ionic current and fluorescence signal from fourteen such experiments are very similar; $\tau = 2.7 \pm 0.2$ and $\tau = 1.9 \pm$

0.2 s, respectively. On repolarization to the holding potential, the ionic currents rapidly deactivate and channels recover from inactivation. Again, these gating events are reported by the fluorophore (Fig. 3C). On repolarization, the fluorescence returns towards baseline and shows a fast phase that has a τ of 87 ± 15 ms and reflects the time course of the return of the voltage sensor during channel deactivation, and a slow phase that has a τ of 739 ± 82 ms, which reflects the slower return of the voltage sensor to its resting state following stabilization of its activated conformation during inactivation (Loots and Isacoff, 1998; Cha and Bezanilla, 1997).

The second site that was labeled to report on inactivation was S424C in the outer pore region. TMRM attached at this site faithfully reports the conformational changes of the pore that are associated with both the onset of and recovery from inactivation (Loots and Isacoff, 1998). Fig. 3D shows ionic currents and fluorescence signals recorded from TMRM-labeled *Shaker* S424C channels. As for *Shaker* A359C, the fluorescence trace in control conditions shows two distinct phases: a fast phase that occurs with a time course similar to activation and which represents 23 ± 2 % of the signal, and a slow phase that occurs with a time course similar to inactivation and which represents 77 ± 2 % of the signal (n=7). Traces in Fig. 3E show an overlay of the control current trace and slow fluorescence signal, and illustrates their similar time courses. The τ of ionic current decay was 2.5 ± 0.2 s and that of the fluorescence decay was 3.7 ± 0.5 s (n=14). On repolarization, the fluorescence signal also shows fast and slow phases. The τ of the fast phase reflecting deactivation is 269 ± 40 ms, and that of the slow phase is 5.2 ± 1.1 s (n=5), which is similar to the time course of the recovery from inactivation (τ = 2.7 ± 0.6 s; n=4).

In the presence of 4-AP, there were marked changes in both the ionic currents and fluorophore reports of both A359C and S424C TMRM-labeled mutant channels. The ionic currents are partially blocked and the rate of the decay is apparently reduced. Peak current is

JPET Fast Forward. Published on October 2, 2006 as DOI: 10.1124/jpet.106.110411
This article has not been copyedited and formatted. The final version may differ from this version.

inhibited by 65 ± 6 % at 3 mM 4-AP (*n*=5). Scaling of the ionic traces in the presence of 4-AP to the control trace in each mutant (the dotted lines in Fig. 3A and D) shows that the rate and extent of slow inactivation of ionic current are significantly reduced in the presence of 4-AP. Fluorophore signals during prolonged depolarization recorded in the presence of 4-AP from both channels (Fig. 3A and D) show, for the first time, the conformational changes associated with the inactivation of drug bound channels. 4-AP increases the relative contribution of the fast phase of fluorescence change in *Shaker* A359C channels from 39 ± 3 % to 72 ± 5 % and reduces the contribution of slow secondary fluorescence deflection that was associated with channel inactivation from 61 ± 3 % to 28 ± 5 % (*n*=5; paired *t*-test, P<0.001). This results in a crossover of the fluorescence traces because 4-AP increases the instantaneous fluorescence deflection by 54 ± 29 %, but reduces the deflection at the end of the depolarizing pulse by 28 ± 9 % (Fig. 3A, lower panel). In addition, the fast and slow phases of the return of the fluorescence to baseline on repolarization are markedly accelerated in the presence of 4-AP (Fig. 3C). The fast τ is reduced to 40 ± 1 ms (from 87 ± 15 ms without 4-AP) suggesting that deactivation is enhanced, which is consistent with previous observations that 4-AP abolishes the immobilization of charge return (McCormack et al., 1993; Bouchard and Fedida, 1995; Loboda and Armstrong, 2001), and the slow τ is reduced to 291 ± 21 ms (from 739 ± 82 ms without 4-AP), which is consistent with the view proposed by Castle and co-workers (Castle et al., 1994) that fewer channels inactivate in the presence of 4-AP during the maintained depolarization. In the case of the *Shaker* S424C channel, the fluorescence signal reporting inactivation is reduced by 64 ± 5 % (*n*=4) in the presence of 4-AP (Fig. 3D, lower panel). An increase in the fast phase is not observed with *Shaker* S424C, probably because the fluorophore at this position does not report as well on activation (Loots and Isacoff, 1998). Interestingly, the time constants of the fast and slow phases

JPET Fast Forward. Published on October 2, 2006 as DOI: 10.1124/jpet.106.110411
This article has not been copyedited and formatted. The final version may differ from this version.

of the return of the fluorescence signal upon repolarization are not different from those in the absence of 4-AP (Fig. 3F). The τ of the fast phase is 181 ± 23 ms and that of the slow phase is 6.1 ± 1.0 s (*n*=5).

Taken together, these current and fluorescence data, which allow direct real-time observation of the conformational changes associated with inactivation, confirm that channel inactivation is greatly reduced after 4-AP binding.

In order to examine the interdependence of 4-AP block and P/C-type channel inactivation further, the effect of 4-AP binding to T449V and W434F channels was examined. Data in Fig. 4A show ionic currents and fluorescence signals recorded during 7 s depolarizing pulses to +60 mV from a holding potential of -80 mV. As suggested earlier (Fig. 2), the T449V mutation largely prevents inactivation, although some current decay does still persist during a long depolarizing pulse (τ = 4.4 ± 0.7 s and the relative amplitude of the decaying component, *a* = 0.22 ± 0.03 in *Shaker* T449V A359C compared with τ = 2.5 ± 0.2 s and *a* = 0.69 ± 0.03 in *Shaker* A359C; *n*=5; P<0.01, *t*-test). The reduced inactivation of T449V mutant channels is accompanied by a slowed and reduced fluorescence decay (τ = 2.4 ± 0.3 s compared with τ = 1.9 ± 0.2 s without the mutation; *n*=5-16). Similar to *Shaker* A359C channels, 3 mM 4-AP blocked *Shaker* T449V A359C ionic current by 76 ± 2 % (Fig. 4A). However, the fluorophore report shows that 4-AP has a much smaller effect on both the fast and slow phases of fluorescence deflection. The extent of the divergence of the fluorescence traces is reduced, because 4-AP increases the instantaneous fluorescence deflection only 21 ± 7 % (compared with 54 ± 29 % in the absence of 4-AP) and reduces the deflection at the end of the pulse by only 13 ± 12 % (compared with 28 ± 9 % in the absence of 4-AP). These data suggest that the reduced inactivation of the T449V mutant diminishes the scope for the effect of 4-AP on the fluorescence

JPET Fast Forward. Published on October 2, 2006 as DOI: 10.1124/jpet.106.110411
This article has not been copyedited and formatted. The final version may differ from this version.

signals. The reduction of the small slow fluorescence deflection from *Shaker* T449V A359C in the presence of 4-AP (Fig. 4A) is probably due to inhibition of the residual inactivation present in these mutant channels. The fast phase of the fluorescence return of *Shaker* T449V A359C channels is still accelerated by 4-AP, from 43 ± 9 to 9 ± 1 ms (n=3), because 4-AP enhances deactivation, and the τ of the slow phase of the fluorescence return is also reduced from 775 ± 132 to 377 ± 56 ms (n=3). These data show that 4-AP can block currents from inactivation-reduced T449V channels equivalently to A359C channels, and that 4-AP can still inhibit the residual inactivation present in T449V channels although the fluorescence report is much less altered by 4-AP in these channels.

In permanently inactivated W434F channels, ionic currents cannot be recorded (Figs. 2G and 4C). Despite this, depolarization produces rapid quenching of the large TMRM fluorescence signal from A359C. As described in Fig. 2, the fluorophore reports very little secondary slow phase and Fig. 4C shows that this is the case even during 7 s depolarizing pulses. The contribution of the fast phase to the total fluorescence is 95 ± 2 % (Fig. 4C). The application of 4-AP has no effect on the kinetics of fluorophore movement during the depolarization except for a small reduction in the absolute signal. In the presence of 3 mM 4-AP, the fast phase contributes 90 ± 4 % to the total deflection (n=3), which is not different from that without 4-AP. As in *Shaker* A359C channels (Fig. 3C), 4-AP accelerates the fast phase of the return of the fluorescence signal on repolarization (Fig. 4D). The τ of the fast phase is reduced from 49 ± 15 ms in the absence to 23 ± 1 ms in the presence of 3 mM 4-AP (n=3), which is consistent with the previous observation that 4-AP abolishes immobilization of the voltage sensor of W434F channels on repolarization (McCormack et al., 1993). Although there is no slow secondary fluorescence deflection from W434F channels during a 7 s depolarization, the recovery of the

JPET Fast Forward. Published on October 2, 2006 as DOI: 10.1124/jpet.106.110411
This article has not been copyedited and formatted. The final version may differ from this version.

fluorescence signal on repolarization shows a slow phase with a τ of 474 ± 3 ms that likely represents the recovery of channels that become C-type inactivated during the voltage pulse. This is consistent with previous observations that P-type inactivated W434F channels are able to undergo C-type inactivation during prolonged depolarization (Olcese et al., 1997). Interestingly, 4-AP accelerates the slow phase of fluorescence return on repolarization (Fig. 4D). The τ of the slow phase of fluorescence return is reduced to 167 ± 65 ms in the presence of 3 mM 4-AP (*n*=3). The incomplete return of the fluorescence signal to the baseline in this case may reflect minor bleaching of the signal rather than incomplete voltage sensor return and this is supported by the evidence of similar incomplete fluorescence return observed in other previous records (e.g., Loots and Isacoff, 1998). These data suggest that 4-AP may be able to bind to P-type inactivated channels and inhibit, at least in part, the transition to C-type inactivation.

The onset of 4-AP block detected by changes in Shaker A359C TMRM fluorescence

As described in Fig. 3A, 4-AP introduces a crossover of the fluorescence signals from *Shaker* A359C channels in the early stages of a maintained depolarization. To investigate this phenomenon further, we measured the effect of different concentrations of 4-AP on the ionic current and fluorescence report during 200 ms voltage pulses to +60 mV (Fig. 5A). In each case in Fig. 5A, the control trace in the absence of 4-AP is shown along with the first and fifth pulses (at 0.2 Hz) after a 3 min application of the indicated concentration of 4-AP during which channels were held closed (holding potential -80 mV). It has been shown that block cannot occur until a channel is opened for the first time (first pulse) in the presence of the drug (Choquet and Korn, 1992; McCormack et al., 1994; Bouchard and Fedida, 1995). Steady-state block is reached by the fifth pulse in each case. In the presence of 0.3 mM 4-AP, the peak ionic current amplitude on the first pulse is not different from that of control, but there is a slow decline in the

current during the pulse that represents the onset of channel block (Fig 5A, left). The fluorescence signals in Fig. 5A accurately report the gating events associated with this onset of channel block. The instantaneous fluorescence signal recorded on the first pulse in the presence of 0.3 mM 4-AP (Fig. 5A, right) is identical to that in control conditions, both in terms of amplitude and kinetics, and is followed by a clear decrease of fluorescence that coincides with the decline of ionic current, and saturates once steady-state block is reached by the fifth pulse (Fig. 5A, right). Increasing concentrations of 4-AP exaggerate both the decay of the ionic current and the increase of the fluorescence signal (Fig. 5A). Since 4-AP does not significantly quench TMRM directly (see Discussion), these data suggest that binding of 4-AP directly increases the fluorescence signal from *Shaker* A359C channels during short depolarizations by inhibiting ongoing inactivation in channels that normally occurs once they open. This allows the fast phase of fluorescence from opening channels to be more completely detected. Consistent with this, in a different set of experiments measuring the onset of block during 7 s pulses, the contribution of the fast phase increases and of the slow phase decreases by 3 ± 1 % with 0.3 mM 4-AP, 4 ± 3 % with 1 mM, 10 ± 2 % with 3 mM and 14 ± 1 % with 10 mM (n=3-4; when compared with the amplitudes of the fast and slow phases in the absence of 4-AP).

Concentration-response curves calculated from steady-state currents at +60 mV, such as those shown in Fig. 5A are shown in Fig. 5B. 4-AP inhibits ionic current with an IC_{50} of 1.3 ± 0.1 mM and a Hill coefficient, n of 0.92 ± 0.05 (n=3-6). This is similar to our own measurements as well as previous reports of 4-AP block of *Shaker* channels that lack an engineered cysteine residue and TMRM dye molecule in *Xenopus* oocytes, which suggest an IC_{50} of ~0.1-0.3 mM (McCormack et al., 1991; Castle et al., 1994), but suggests that the A359C mutation and its attached TMRM molecule may alter 4-AP potency to a small degree. The effect

JPET Fast Forward. Published on October 2, 2006 as DOI: 10.1124/jpet.106.110411
This article has not been copyedited and formatted. The final version may differ from this version.

of different concentrations of 4-AP on the steady-state conductance- and fluorescence-voltage relationships is shown in Figs. 5C and D. These data are taken from currents and fluorescence reports recorded during 200 ms voltage pulses from -100 to +80 mV. It is clear that increasing the concentration of 4-AP shifts the conductance-voltage relation of *Shaker* A359C channels to more depolarized potentials and also reduces the maximal conductance (Fig. 5C). This is consistent with the previous suggestion that 4-AP binding stabilizes the activated-not-open state of the channel (McCormack et al., 1994; del Camino et al., 2005) where the voltage sensor charges have moved, but the concerted opening step is prevented (Pathak et al., 2005). In agreement with this, Fig. 5D shows that 4-AP has no effect on the $V_{1/2}$ of the fluorescence-voltage relationship suggesting that 4-AP has little effect on voltage sensor movement and that 4-AP bound channels gate normally without significant opening as suggested previously (McCormack et al., 1994;Armstrong and Loboda, 2001). The fluorescence-voltage relationships also show the concentration-dependent increase in the absolute fluorescence signal amplitude seen in the presence of 4-AP in Figs. 3A and 5A without any change in the voltage-dependence of the signal. This suggests that the additional fluorescence signal does indeed reflect activation of channels.

4-AP stabilizes the activated-not-open state

The ILT mutant *Shaker* channel provides a useful tool in channel gating studies because it isolates voltage sensor movement from the cooperative opening transition of channels, i.e., a pulse to 0 mV, for example, will move most of the gating charge, but does not culminate in channel opening (Smith-Maxwell et al., 1998a, b; see also Fig. 1B). This state was recently described as the activated-not-open state (del Camino et al., 2005) and is suggested to be the same state that is stabilized by the binding of 4-AP. We reasoned that the fluorophore report

from the ILT mutant channel at 0 mV should therefore be identical to that from 4-AP bound channels and also insensitive to 4-AP. Fig. 6A shows current traces and fluorescence signals recorded from *Shaker* ILT A359C channels during a 7 s pulse to 0 mV from a holding potential of -80 mV in the absence and presence of 3 mM 4-AP. Fig. 6B shows *G-V* and *F-V* curves plotted from 100 ms pulses over a wide range of potentials. It is clear that at 0 mV, the ILT mutant channels do not open, since there is no observable current, but that the majority of the charge has moved, since the fluorophore reports a rapid and large conformational change. Fig. 6B shows that the $V_{1/2}$ of the *G-V* and *F-V* curves of the *Shaker* ILT A359C channel are separated by more than 150 mV and that opening occurs only at very depolarized potentials. The fluorescence report at 0 mV in the absence of 4-AP shows no secondary movement following the conformational changes associated with charge movement (Fig. 6A) as it does in the *Shaker* A359C channel in the presence of 4-AP (Fig. 3A). Furthermore, 4-AP does not alter the fluorescence report at 0 mV (Fig. 6A). The similarity between the fluorophore reports from 4-AP bound channels and the ILT mutant channels is consistent with the idea that 4-AP, like the ILT mutant, stabilizes the activated-not-open state of the channel. The lack of evidence of an inactivation transition in the fluorescence trace at 0 mV in the absence of 4-AP also supports the argument that inactivation is strictly coupled to opening in this channel.

JPET Fast Forward. Published on October 2, 2006 as DOI: 10.1124/jpet.106.110411
This article has not been copyedited and formatted. The final version may differ from this version.

Discussion:

4-AP bound channels cannot inactivate

The fluorescence emission of TMRM attached to A359C in the S3-S4 linker reports a fast decrease, followed by a slower declining phase on depolarization that reflect activation and inactivation gating conformational changes, respectively (Fig. 2). It is clear that the report from this position is very sensitive to inactivation gating because a slow fluorescence decay can be observed not only during prolonged depolarization (Fig. 3A) when the majority of channels inactivate, but also during short pulses (Fig. 2B) when only a small proportion of channels enter the inactivated conformation. We therefore used the fluorescence report from *Shaker* A359C channels to investigate the effect of 4-AP on channel inactivation, because although the effect of 4-AP binding on voltage sensor movement has been extensively studied (McCormack et al., 1994; Bouchard and Fedida, 1995; Armstrong and Loboda, 2001), there is only one report of the effect on inactivation of ionic current, which suggested that inactivation and 4-AP binding are mutually exclusive (Castle et al., 1994). Using the secondary slow phase of fluorescence deflection from *Shaker* A359C, as well as the slow report from *Shaker* S424C channels, we have shown directly that 4-AP inhibits the conformational changes associated with inactivation gating of *Shaker* channels (Fig. 3). In support of this conclusion, the effect of 4-AP on the slow secondary fluorescence deflection that reflects inactivation was reduced in mutant channels with reduced (T449V; Fig. 4A) or permanent (W434F; Fig. 4C) inactivation.

Although it is possible that changes in the fluorescence on 4-AP binding are due to inhibition of ion conduction and that K^+ permeation alters the fluorescence report, evidence suggests that this is not the case: 1) on repolarization ionic current reverses direction (as seen in Fig. 3A), but the fluorescence report does not as would be expected if ion conduction was a

JPET Fast Forward. Published on October 2, 2006 as DOI: 10.1124/jpet.106.110411
This article has not been copyedited and formatted. The final version may differ from this version.

major determinant of the fluorescence signal; 2) previously, Loots and Isacoff (1998) showed that the rate of the slow fluorescence report is highly dependent on modifications that alter the rate of inactivation of ionic current, for example, low pH enhances inactivation and the fluorescence decay whilst high K^+ slows inactivation and the fluorescence decay. Consistent with this, the T449V mutation used in the present study (Fig. 4A) slows ionic inactivation and reduces the slow fluorescence decay. Taken together, these data suggest that the fluorescence reports in the present study faithfully report activation and inactivation and are not altered by ion permeation. A similar conclusion was reached by Cha and Bezanilla (1997) who demonstrated that TEA and Agitoxin block of the pore altered the fluorescence report from A359C, but that this was not due to inhibition of ion conduction, but rather that the blocking particles prevented conformational changes associated with channel opening.

4-AP can bind to P-type inactivated channels

Using conventional electrophysiological approaches, Castle et al. (1994) showed that 4-AP slows inactivation of *Shaker* channels and suggested that 4-AP cannot bind inactivated channels. However, it was not possible in these experiments to separate the effects of 4-AP on P-type inactivation from those on C-type inactivation. In the present study, we have directly observed the effect of 4-AP on P-type inactivation by using the W434F permanently P-type inactivated mutant channel as well as the effect of 4-AP on C-type inactivation by analyzing the return of the fluorescence signal to baseline upon repolarization, which represents the extent of stabilization of the voltage sensor in its activated conformation, a hallmark of C-type inactivation. W434F channels display almost identical gating currents to wild-type channels, but do not conduct K^+ due to permanent P-type inactivation (Yang et al., 1997). Despite this,

channels are thought to be able to access the C-type inactivated state on depolarization because they still exhibit charge immobilization following maintained depolarization (Olcese et al., 1997). In the present study, we observed that the return of the fluorescence signal to baseline on repolarization was enhanced in the presence of 4-AP (Fig. 4D). These data suggest that 4-AP can bind to P-type inactivated channels and inhibit their progression to the C-type inactivated state (see Fig. 1B). Since 4-AP can only access its binding site in the *Shaker* channel when the intracellular gate is open, these data show that, although W434F channels are permanently inactivated, the intracellular gate opens with similar voltage dependence to that in conducting channels, which is consistent with the previous observation that the tetraethylammonium binding site is also available on depolarization (Perozo et al., 1993). This conclusion is also consistent with a number of previous studies in which 4-AP is clearly seen to modify gating currents in W434F mutant channels (e.g. McCormack et al., 1994; Bouchard and Fedida, 1995; Loboda and Armstrong, 2001). From our data, we cannot determine whether 4-AP can bind to C-type inactivated channels. If not, this may be consistent with the inability of 4-AP to bind inactivated channels following the very long pulses used by Castle et al. (1994) that presumably drive most channels to the C-type inactivated state.

Inactivation results in underestimation of voltage sensor movement

When comparing the fluorescence report from *Shaker* A359C in the absence and presence of 4-AP, we observed a prominent crossover early on in the depolarizing pulse (Fig. 3A). This was reflected as an enhancement of the fluorescence signal during 200 ms pulses (Fig. 5A) suggesting that 4-AP block resulted in an increased quenching of TMRM during depolarization. However, a number of observations suggest that it is unlikely that the increased

JPET Fast Forward. Published on October 2, 2006 as DOI: 10.1124/jpet.106.110411
This article has not been copyedited and formatted. The final version may differ from this version.

amplitude of deflection is due to a non-specific quenching of the TMRM fluorophore by the drug: 1) the basal level of fluorescence emission was the same in the presence and absence of 4-AP, i.e. the increase in the fluorescence signal amplitude only occurs once the channel is opened and 4-AP is allowed to bind; 2) addition of 4-AP to oocytes expressing channels with no accessible external cysteine residue (i.e. *Shaker* Δ6-46 C245V channels) had no effect on fluorophore emission (data not shown); and, 3) emission intensities recorded on excitation of TMRM dye in solution with or without 3 mM 4-AP were not different (data not shown). Instead, we conclude that the increased fluorescence deflection seen during the short pulses in Fig. 5A and the crossover of the fluorescence traces in Fig. 3A is a consequence of the 4-AP-induced inhibition of inactivation. The peak of the fluorescence trace in the absence of 4-AP is underestimated due to the onset of inactivation, which results in a slow secondary phase of fluorescence. Since 4-AP binding greatly reduces the ability of *Shaker* channels to inactivate, this slow phase is almost abolished resulting in an increase in the amplitude of the fast phase of fluorescence. In support of this conclusion, the slow phase of the fluorescence decay in the presence of 4-AP and the divergence of the fluorescence trace from that in control conditions is reduced in the inactivation-deficient T449V mutant (Fig. 4A).

4-AP stabilizes the activated-not-open state

It is well established from gating current studies in *Shaker* channels that 4-AP binding does not alter the early independent gating transitions between closed states (McCormack et al., 1994; Armstrong and Loboda, 2001). Consistent with this, we have shown that the fast fluorescence report from fluorophores attached in the S3-S4 linker at position A359C, is largely unaltered by the binding of 4-AP (Figs. 2B and 5D). It was recently suggested that, like the ILT

mutation, 4-AP promotes the activated-not-open state of the channel (Armstrong and Loboda, 2001; del Camino et al., 2005). In the present study, the fluorophore report from ILT mutant channels recorded during a maintained depolarization to 0 mV, which activates channels and moves the voltage sensor (Smith-Maxwell et al., 1998a, b), but does not open channels, mimicked that recorded from normally activating channels in the presence of 4-AP (compare Figs. 3A and 6A). Furthermore, application of 4-AP did not alter this report (Fig. 6). These data support the conclusion that 4-AP binding promotes the activated-not-open channel conformation (del Camino et al., 2005).

References:

Armstrong CM and Loboda A (2001) A model for 4-aminopyridine action on K channels: Similarities to tetraethylammonium ion action. *Biophys J* **81**:895-904.

Bever CT, Jr., Anderson PA, Leslie J, Panitch HS, Dhib-Jalbut S, Khan OA, Milo R, Hebel JR, Conway KL, Katz E, and Johnson KP (1996) Treatment with oral 3,4 diaminopyridine improves leg strength in multiple sclerosis patients: results of a randomized, double-blind, placebo-controlled, crossover trial. *Neurology* **47**:1457-1462.

Bezanilla F (2002) Voltage sensor movements. *J Gen Physiol* **120**:465-473.

Bouchard RA and Fedida D (1995) Closed and open state binding of 4-aminopyridine to the cloned human potassium channel Kv1.5. *J Pharmacol Exp Ther* **275**:864-876.

Castle NA, Fadous SR, Logothetis DE, and Wang GK (1994) 4-aminopyridine binding and slow inactivation are mutually exclusive in rat Kv1.1 and *Shaker* potassium channels. *Mol Pharmacol* **46**:1175-1181.

Cha A and Bezanilla F (1997) Characterizing voltage-dependent conformational changes in the *Shaker* K^+ channel with fluorescence. *Neuron* **19**:1127-1140.

Choquet D and Korn H (1992) Mechanism of 4-aminopyridine action on voltage-gated potassium channels in lymphocytes. *J Gen Physiol* **99**:217-240.

Claydon TW, Boyett MR, Sivaprasadarao A, Ishii K, Owen JM, O'Beirne HA, Leach R, Komukai K, and Orchard CH (2000) Inhibition of the K^+ channel Kv1.4 by acidosis: protonation of an extracellular histidine slows the recovery from N-type inactivation. *J Physiol* **526**:253-264.

DeBiasi M, Hartmann HA, Drewe JA, Taglialatela M, Brown AM, and Kirsch GE (1993) Inactivation determined by a single site in K^+ pores. *Pflueg Arch* **422**:354-363.

del Camino D, Kanevsky M, and Yellen G (2005) Status of the intracellular gate in the activated-not-open state of shaker K^+ channels. *J Gen Physiol* **126**:419-428.

Gonzalez C, Rosenman E, Bezanilla F, Alvarez O, and Latorre R (2001) Periodic perturbations in *Shaker* K^+ channel gating kinetics by deletions in the S3-S4 linker. *Proc Natl Acad Sci USA* **98**:9617-9623.

Grissmer S, Nguyen AN, Aiyar J, Hanson DC, Mather RJ, Gutman GA, Karmilowicz MJ, Auperin DD, and Chandy KG (1994) Pharmacological characterization of five cloned voltage-gated K^+ channels, types Kv1.1, 1.2, 1.3, 1.5, and 3.1, stably expressed in mammalian cell lines. *Mol Pharmacol* **45**:1227-1234.

Hoshi T, Zagotta WN, and Aldrich RW (1990) Biophysical and molecular mechanisms of *Shaker* potassium channel inactivation. *Science* **250**:533-538.

Hoshi T, Zagotta WN, and Aldrich RW (1991) Two types of inactivation in *Shaker* K^+ channels: Effects of alterations in the carboxy-terminal region. *Neuron* **7**:547-556.

Kehl SJ (1990) 4-Aminopyridine causes a voltage-dependent block of the transient outward K^+ current in rat melanotrophs. *J Physiol* **431**:515-528.

Kirsch GE and Drewe JA (1993) Gating-dependent mechanism of 4-aminopyridine block in two related potassium channels. *J Gen Physiol* **102**:797-816.

Kirsch GE and Narahashi T (1983) Site of action and active form of aminopyridines in squid axon membranes. *J Pharmacol Exp Ther* **226**:174-179.

Kirsch GE, Yeh JZ, and Oxford GS (1986) Modulation of aminopyridine block of potassium currents in squid axon. *Biophys J* **50**:637-644.

Kurata HT and Fedida D (2006) A structural interpretation of voltage-gated potassium channel inactivation. *Prog Biophys Mol Biol* **92**:185-208.

Loboda A and Armstrong CM (2001) Resolving the gating charge movement associated with late transitions in K channel activation. *Biophys J* **81**:905-916.

Loots E and Isacoff EY (1998) Protein rearrangements underlying slow inactivation of the *Shaker* K^+ channel. *J Gen Physiol* **112**:377-389.

Loots E and Isacoff EY (2000) Molecular coupling of S4 to a K^+ Channel's slow inactivation gate. *J Gen Physiol* **116**:623-636.

Lopez-Barneo J, Hoshi T, Heinemann SH, and Aldrich RW (1993) Effects of external cations and mutations in the pore region on C-type inactivation of Shaker potassium channels. *Receptors and Channels* **1**:61-71.

Mannuzzu LM, Moronne MM, and Isacoff EY (1996) Direct physical measurement of conformational rearrangement underlying potassium channel gating. *Science* **271**:213-216.

McCormack K, Tanouye MA, Iverson LE, Lin JW, Ramaswami M, McCormack T, Campanelli JT, Mathew MK, Rudy B (1991) A role for hydrophobic residues in the voltage-dependent gating of Shaker K^+ channels. *Proc Natl Acad Sci USA* **88**:2931-2935.

McCormack K, Joiner WJ, and Heinemann SH (1994) A characterization of the activating structural rearrangements in voltage-dependent *Shaker* K^+ channels. *Neuron* **12**:301-315.

Olcese R, Latorre R, Toro L, Bezanilla F, and Stefani E (1997) Correlation between charge movement and ionic current during slow inactivation in *Shaker* K^+ channels. *J Gen Physiol* **110**:579-589.

Pathak M, Kurtz L, Tombola F, and Isacoff E (2005) The Cooperative Voltage Sensor Motion that Gates a Potassium Channel. *J Gen Physiol* **125**:57-69.

Perozo E, MacKinnon R, Bezanilla F, and Stefani E (1993) Gating currents from a non-conducting mutant reveal open-closed conformation in Shaker K^+ channels. *Neuron* **11**:353-358.

Ray EC and Deutsch C (2006) A trapped intracellular cation modulates K^+ channel recovery from slow inactivation. *J Gen Physiol* **128**:203-217.

Shieh CC, Klemic KG, and Kirsch GE (1997) Role of transmembrane segment S5 on gating of voltage-dependent K^+ channels. *J Gen Physiol* **109**:767-778.

Shieh C-C and Kirsch GE (1994) Mutational analysis of ion conduction and drug binding sites in the inner mouth of voltage-gated K^+ channels. *Biophys J* **67**:2316-2325.

Smith-Maxwell CJ, Ledwell JL, and Aldrich RW (1998a) Role of the S4 in cooperativity of voltage-dependent potassium channel activation. *J Gen Physiol* **111**:399-420.

Smith-Maxwell CJ, Ledwell JL, and Aldrich RW (1998b) Uncharged S4 residues and cooperativity in voltage-dependent potassium channel activation. *J Gen Physiol* **111**:421-439.

Starkus JG, Kuschel L, Rayner MD, and Heinemann SH (1998) Macroscopic Na^+ currents in the "nonconducting" *Shaker* potassium channel mutant W434F. *J Gen Physiol* **112**:85-93.

Thompson S (1982) Aminopyridine block of transient potassium current. *J Gen Physiol* **80**:1-18.

Tseng GN, Jiang M, and Yao JA (1996) Reverse use dependence of Kv4.2 blockade by 4-aminopyridine. *J Pharmacol Exp Ther* **279**:865-876.

Wolfe DL, Hayes KC, Hsieh JT, and Potter PJ (2001) Effects of 4-aminopyridine on motor evoked potentials in patients with spinal cord injury: a double-blinded, placebo-controlled crossover trial. *J Neurotrauma* **18**:757-771.

Yang YS, Yan YY, and Sigworth FJ (1997) How does the W434F mutation block current in *Shaker* potassium channels. *J Gen Physiol* **109**:779-789.

Yao J-A and Tseng G-N (1994) Modulation of 4-AP block of a mammalian A-type K channel clone by channel gating and membrane voltage. *Biophys J* **67**:130-142.

Yellen G (1998) The moving parts of voltage-gated ion channels. *Q Rev Biophys* **31**:239-295.

Footnotes:

TWC and MV contributed equally to the manuscript.

This work was supported by grants from the Heart and Stroke Foundations of British Columbia and Yukon and the CIHR to DF and SJK. S.R. was supported by a University of British Columbia Graduate Fellowship. T.W.C was supported by a postdoctoral research fellowship funded by a Focus on Stroke strategic initiative from The Canadian Stroke Network, the Heart and Stroke Foundation, the CIHR Institute of Circulatory and Respiratory Health and the CIHR/Rx&D Program along with AstraZeneca Canada.

Figure Legends:

Figure 1. Relevant sites within the *Shaker* channel and kinetic scheme of the action of 4-AP. Cartoon of the *Shaker* channel (A) with amino acid positions that are relevant to the present study highlighted. The native cysteine residue in the S1-S2 linker was replaced with a valine residue (C245V). W434F and T449V were used to modify inactivation. TMRM was attached at A359C in the S3-S4 linker or S424C in the outer pore. The molecular structures of 4-AP and TMRM are also shown. A 4-AP molecule is ~2.4 Å wide and ~3.6 Å long. The diameter of the inner vestibule of the pore is ~12 Å. A TMRM molecule is ~14 Å across. Kinetic scheme for the action of 4-AP (B) modified from that of Armstrong and Loboda (2001). C_0 to C_4 represent closed states of the channel and O represents the open state. Transitions between C_0 and C_4 represent voltage-dependent, early independent gating transitions and the transition from C_4 to O (*) represents the weakly voltage-dependent, final concerted opening. Hence, C_4 can be considered the recently described activated-not-open state (del Camino and Yellen, 2005; Pathak et al., 2005). 4-AP can only bind when channels open, and once bound the drug strongly biases the closed 4-AP bound state ($C_{4,AP}$). 4-AP bound channels are able to undergo the independent transitions ($C_{0,AP}$ to $C_{4,AP}$), but the drug retards the transition to opening. Inactivation gating transitions from the open state shown are as suggested previously (Loots and Isacoff, 1998). I_P and I_C represent P- and C-type inactivated states, respectively. The dashed arrows reflect that the transitions made during recovery from inactivation are not known. P-type inactivation from the open state only is shown, although there is evidence for P-type inactivation from rest (Yang et al., 1994). The ability of 4-AP to bind to P-type inactivated channels (I_P to $I_{P,AP}$) is demonstrated in the present study by actions on W434F mutant channels. The fate of $I_{P,AP}$ channels was not

directly addressed in the study so the unbinding transitions from this state have been omitted for reasons of clarity and to avoid undue speculation.

Figure 2. A fluorophore attached at A359C in the *Shaker* channel reports both activation and inactivation. Typical current traces (A, D, G) and fluorescence signals (B, E, H) recorded from *Shaker* A359C channels without or with mutations (T449V or W434F) that affect inactivation properties during 100 ms voltage pulses from -100 to +100 mV from a holding potential of -80 mV. Although pulses were applied in 10 mV increments, only every other pulse is shown for clarity. Dashed lines show extrapolations of single exponential fits (from when ~50 % of the current has activated) to the time course of current activation (A and D) or the fast fluorescence deflection (B, E, H) at +100 mV to highlight the degree of ionic current and fluorescence decay in each channel. (C, F, I) Fast (F_{fast}) and slow (F_{slow}) phases of the fluorescence signals and the activating (*G-V*) and inactivating (I_{inact}) components of the ionic current record plotted as a function of potential (n=4-10). I_{inact} represents the amplitude of the current that decays during the 100 ms pulse. This value at each potential is normalized to that measured at +100 mV. The fluorescence reports from *Shaker* T449V A359C and *Shaker* W434F A359C channels could be fit with a single exponential that represented just the fast phase and therefore F_{slow} is absent. *Shaker* W434F A359C channels were non-conducting and therefore the *G-V* relationship is absent in this mutant.

Figure 3. 4-AP abolishes the inactivation-dependent component of fluorescence. (A and D) Ionic currents (top) and fluorescence signals (bottom) recorded during a 7 s (A) or 42 s (D) depolarizing pulse to +60 mV from *Shaker* A359C (A) or *Shaker* S424C (D) channels from a

holding potential of -80 mV in the absence and presence of 4-AP. The dotted trace represents the normalized ionic current in the presence of 4-AP scaled 2-fold in (A) and 8-fold in (D). (B and E) Superimposition of ionic current and the slow phase of the fluorescence deflection in the absence of 4-AP show similar kinetics. The time constants of ionic current and fluorescence signal decay are 2.5 ± 0.2 and 1.9 ± 0.2 s, respectively (n=16), for *Shaker* A359C in (B) and 2.6 ± 0.3 and 3.8 ± 0.9 s, respectively (n=6-10), for *Shaker* S424C in (E). (C and F) Normalization of the return of the fluorescence signal to baseline on repolarization in the absence and presence of 4-AP from *Shaker* A359C (C) and *Shaker* S424C (F). The return of the fluorescence is biexponential. The fast and slow time constants are 87 ± 15 (relative amplitude, a = 0.64 ± 0.07) and 739 ± 82 ms (a = 0.36 ± 0.07), respectively, in the absence of 4-AP and 40 ± 1 (a = 0.75 ± 0.04) and 291 ± 21 ms (a = 0.25 ± 0.04), respectively, in the presence of 3 mM 4-AP in *Shaker* A359C. The corresponding values in *Shaker* S424C are 269 ± 40 ms (a = 0.39 ± 0.10) and 5.2 ± 1.1 s (a = 0.61 ± 0.10) in the absence of 4-AP and 181 ± 23 ms (a = 0.45 ± 0.10) and 6.1 ± 1.0 s (a = 0.55 ± 0.10) in the presence of 10 mM 4-AP.

Figure 4. Modulation of inactivation alters the effect of 4-AP on *Shaker* A359C TMRM fluorescence. (A and C) Ionic (top) and fluorescence (bottom) traces recorded from *Shaker* T449V A359C inactivation-reduced mutant channels (A) and *Shaker* W434F A359C permanently inactivated channels (C) during a 7 s depolarizing pulse to +60 mV from a holding potential of -80 mV in the absence and presence of 4-AP. The dotted trace in panel A represents the ionic current in the presence of 4-AP scaled 4-fold to match the peak of the control current. (B and D) Normalization of the return of the fluorescence signal on repolarization in the absence and presence of 4-AP from *Shaker* T449V A359C (B) and *Shaker* W434F A359C (D). The fast

JPET Fast Forward. Published on October 2, 2006 as DOI: 10.1124/jpet.106.110411
This article has not been copyedited and formatted. The final version may differ from this version.

and slow time constants are 43 ± 9 (relative amplitude, a = 0.71 ± 0.04) and 775 ± 132 ms (a = 0.29 ± 0.04), respectively, in the absence of 4-AP and 9 ± 1 (a = 0.88 ± 0.05) and 337 ± 56 ms (a = 0.12 ± 0.05), respectively, in the presence of 3 mM 4-AP in *Shaker* T449V A359C. The corresponding values in *Shaker* W434F A359C are 49 ± 15 (a = 0.68 ± 0.05) and 474 ± 3 ms (a = 0.32 ± 0.05) in the absence of 4-AP and 23 ± 1 (a = 0.86 ± 0.06) and 167 ± 65 ms (a = 0.14 ± 0.06) in the presence of 3 mM 4-AP.

Figure 5. The onset of 4-AP block detected by changes in *Shaker* A359C TMRM fluorescence. (A) Ionic currents (left) and fluorescence signals (right) recorded during depolarizing pulses to +60 mV from *Shaker* A359C in the absence of 4-AP (control) and the first and fifth pulses following a 3 min application of 4-AP (the membrane was held at –80 mV during 4-AP application to prevent channel block). (B) 4-AP concentration-response curves generated from the steady-state level of block using ionic currents or fluorescence deflections at +60 mV as shown in panel (A). The IC_{50} and Hill coefficient (n) calculated from the ionic currents are 1.3 ± 0.1 mM and 0.92 ± 0.05, respectively (n=3-6). (C) Conductance-voltage (G-V) relations with increasing concentrations of 4-AP were constructed using the peak current amplitudes during the pulse (n=3-5). $V_{1/2}$ and k values were -10.0 ± 1.8 mV and 20.5 ± 1.5 for control; 3.3 ± 2.6 mV and 26.3 ± 2.0 for 300 μM 4-AP ; 9.7 ± 2.4 mV and 23.9 ± 1.8 for 1 mM 4-AP; 37.9 ± 3.6 mV and 29.0 ± 2.0 for 3 mM 4-AP; 49.3 ± 4.5 mV and 29.1 ± 2.2 for 10 mM 4-AP. These values in the absence of 4-AP are similar to those previously reported for channels with mutations of the S3-S4 linker (Gonzalez et al., 2001) (D) Fluorescence-voltage (F-V) relations were generated by normalizing the peak fluorescence deflections in a given 4-AP concentration to those in the absence of 4-AP in each oocyte (n=3-5). The $V_{1/2}$ and k values were

-26.7 ± 1.5 mV and 26.2 ± 1.3, respectively, for control; -35.5 ± 1.7 mV and 23.2 ± 1.4 for 300 μM 4-AP; -39.0 ± 1.1 mV and 19.7 ± 0.9 for 1 mM 4-AP; -38.0 ± 1.3 mV and 18.0 ± 1.1 for 3 mM 4-AP; -26.9 ± 1.8 mV and 24.2 ± 1.5 for 10 mM 4-AP.

Figure 6. 4-AP binding stabilizes the activated-not-open state of the channel. (A) Ionic (top) and fluorescence (bottom) traces recorded from *Shaker* ILT A359C channels in the absence and presence of 3 mM 4-AP during a 7 s depolarizing pulse to 0 mV (where maximum voltage sensor movement takes places without any channel opening) from a holding potential of -80 mV. (B) Isochronal conductance- and fluorescence-voltage relations generated from normalized peak current and fluorescence deflections plotted as a function membrane potential (n=5). $V_{1/2}$ and k values were 101.1 ± 5.4 mV and 36.8 ± 3.5, respectively, for ionic current and the respective values for the fluorescence deflection were -74.5 ± 0.5 mV and 16.1 ± 0.4.

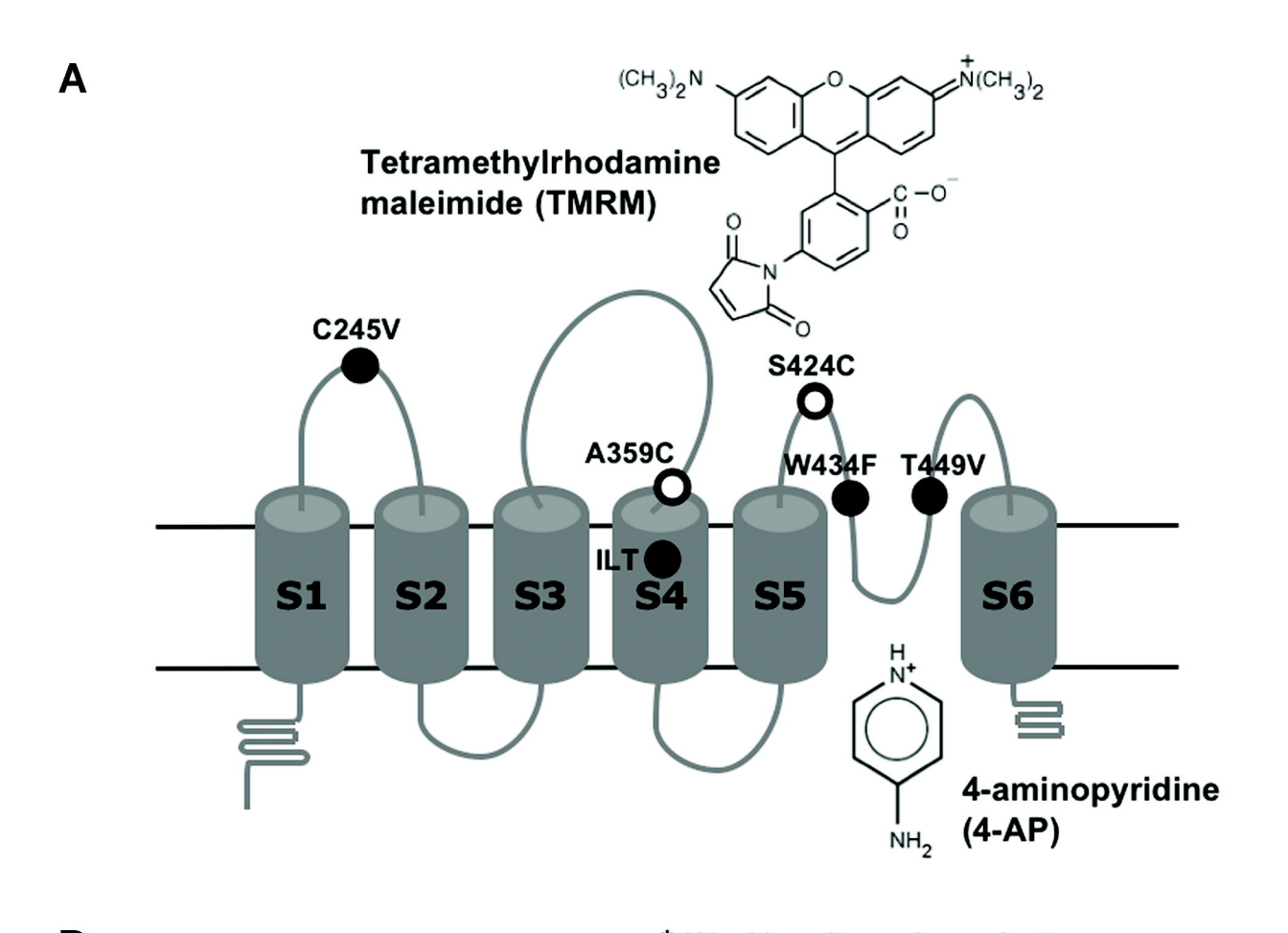
A
Tetramethylrhodamine
maleimide (TMRM)
C245V
S424C
A359C
W434F
T449V
ILT
S1
S2
S3
S4
S5
S6
4-aminopyridine
(4-AP)

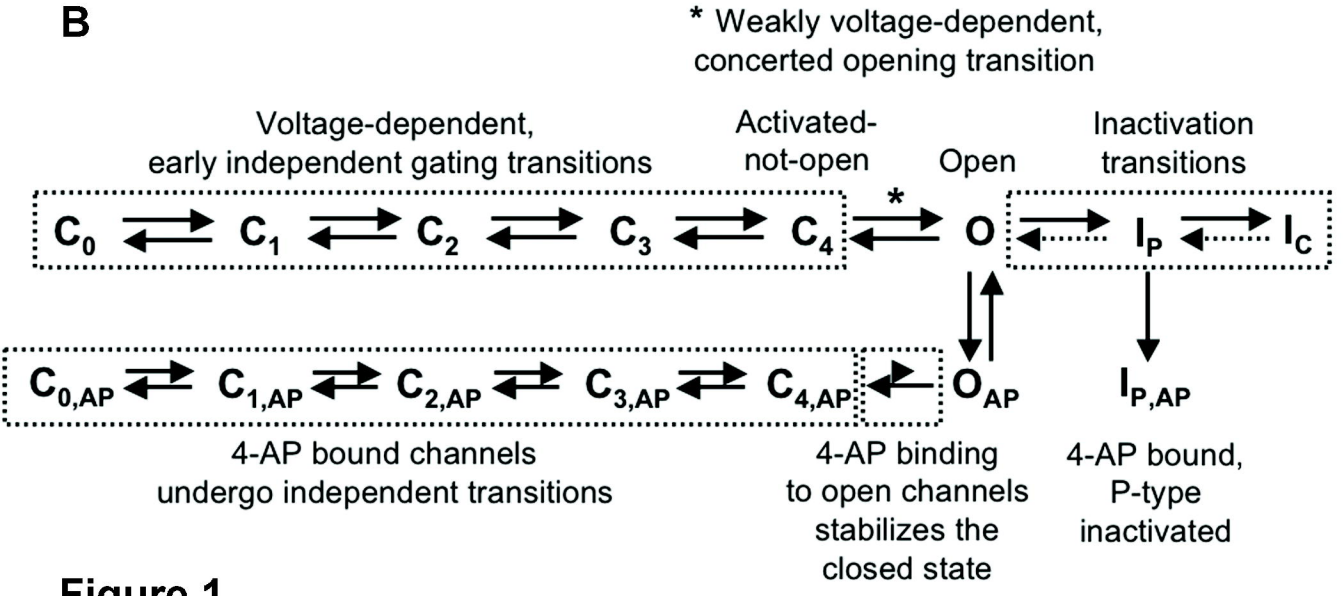
B
* Weakly voltage-dependent,
concerted opening transition
Voltage-dependent,
early independent gating transitions
Activated-
not-open
Open
Inactivation
transitions
C0 C1 C2 C3 C4 * O IP IC
C0,AP C1,AP C2,AP C3,AP C4,AP OAP IP,AP
4-AP bound channels
undergo independent transitions
4-AP binding
to open channels
stabilizes the
closed state
4-AP bound,
P-type
inactivated

Figure 1

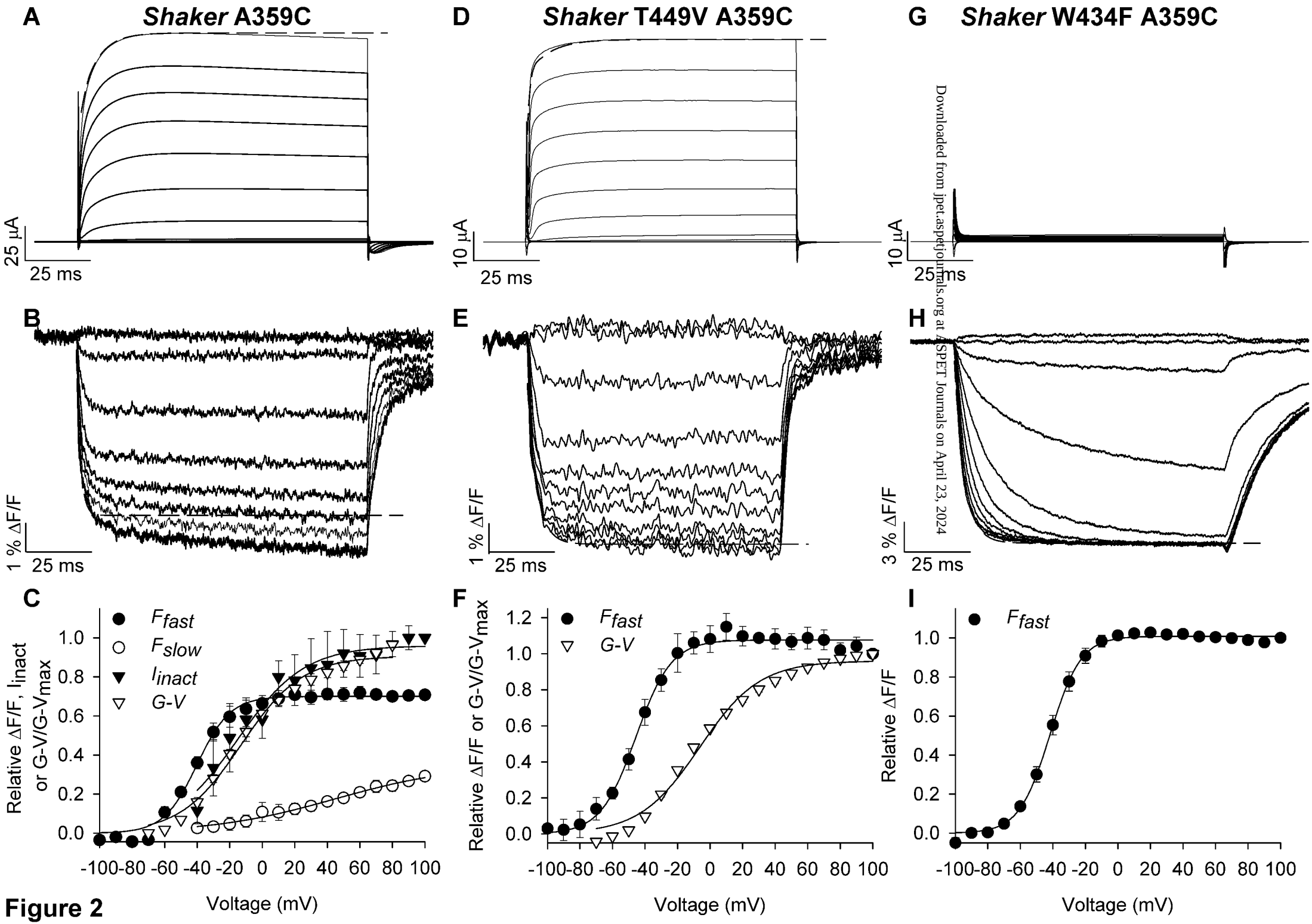

Figure 2

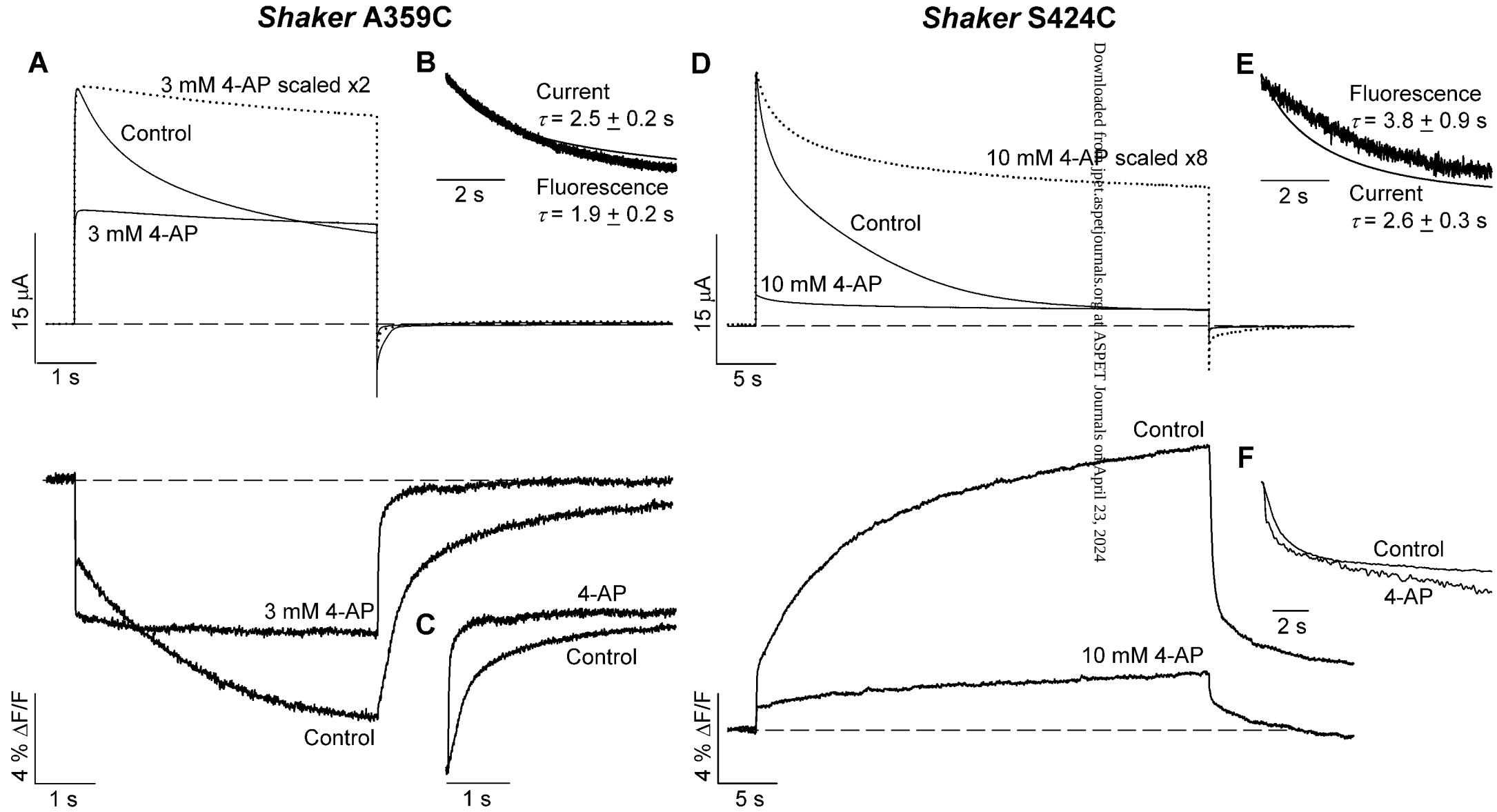

Figure 3

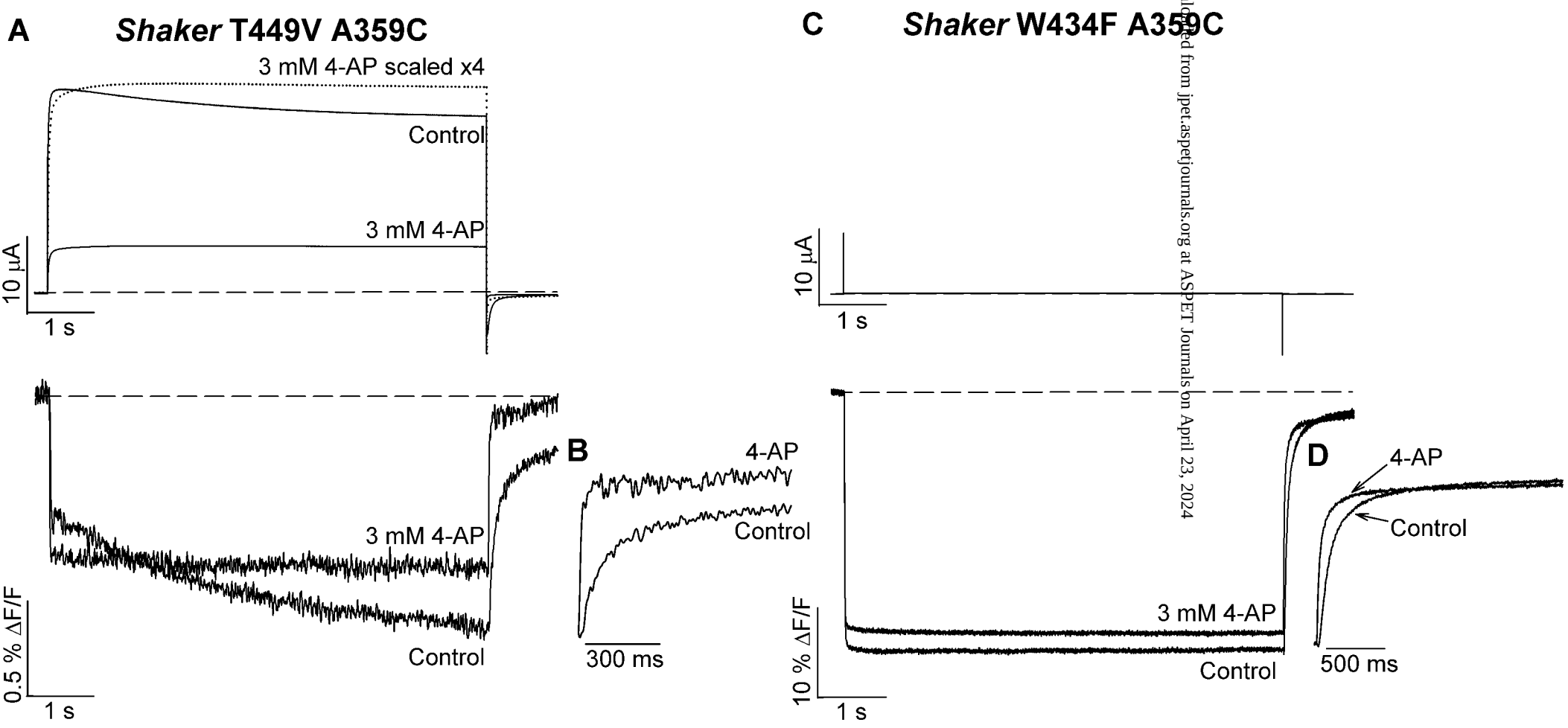

Figure 4

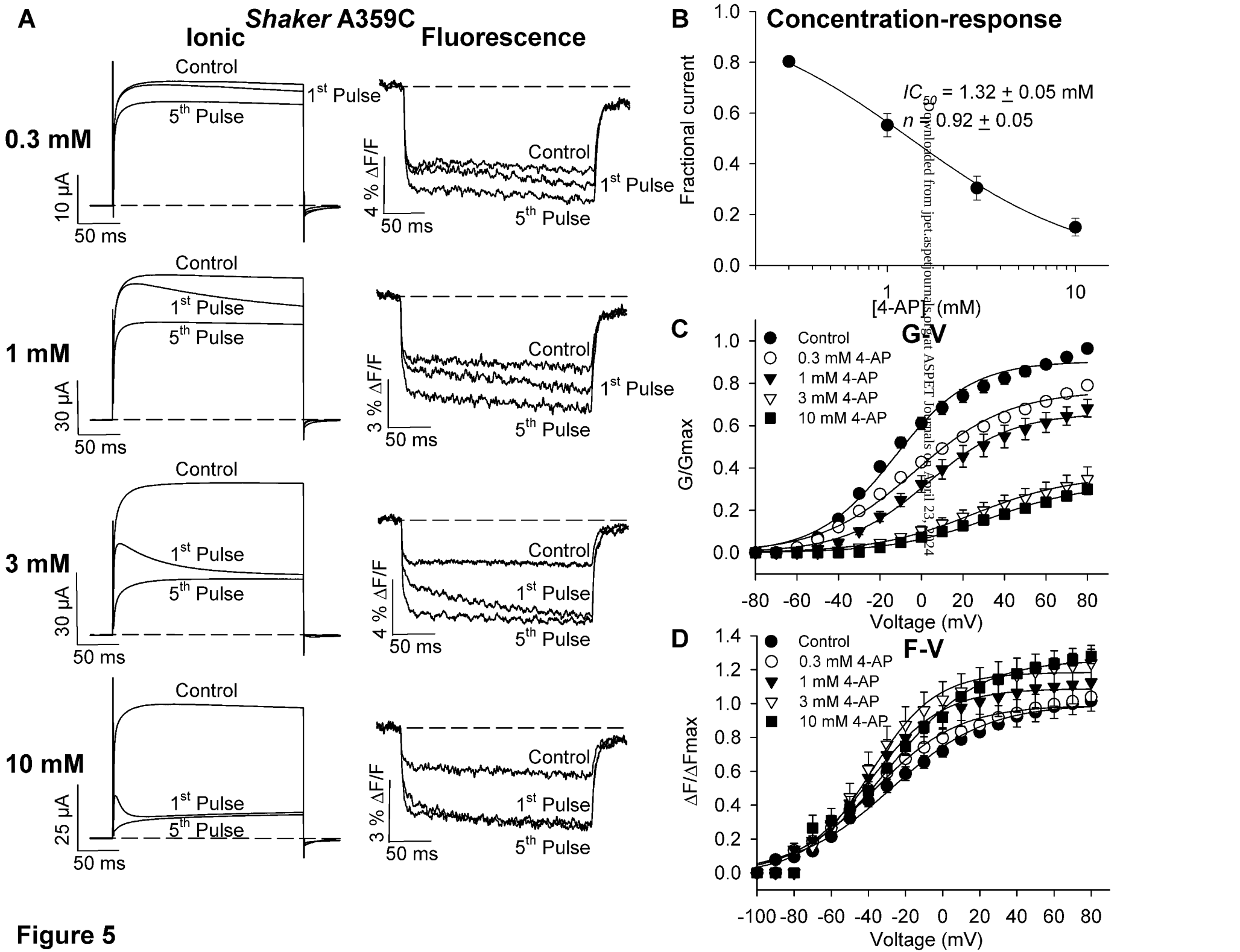
A
Ionic
Shaker A359C
Fluorescence
0.3 mM
Control
1st Pulse
5th Pulse
10 µA
50 ms
4 % ΔF/F
1 mM
30 µA
3 % ΔF/F
3 mM
10 mM
25 µA
B
Concentration-response
Fractional current
IC50 = 1.32 ± 0.05 mM
n = 0.92 ± 0.05
[4-AP] (mM)
C
GV
G/Gmax
0.3 mM 4-AP
1 mM 4-AP
3 mM 4-AP
10 mM 4-AP
Voltage (mV)
D
F-V
ΔF/ΔFmax
Downloaded from jpet.aspetjournals.org at ASPET Journals on April 23, 2024

Figure 5

JPET Fast Forward. Published on October 2, 2006 as DOI: 10.1124/jpet.106.110411
This article has not been copyedited and formatted. The final version may differ from this version.

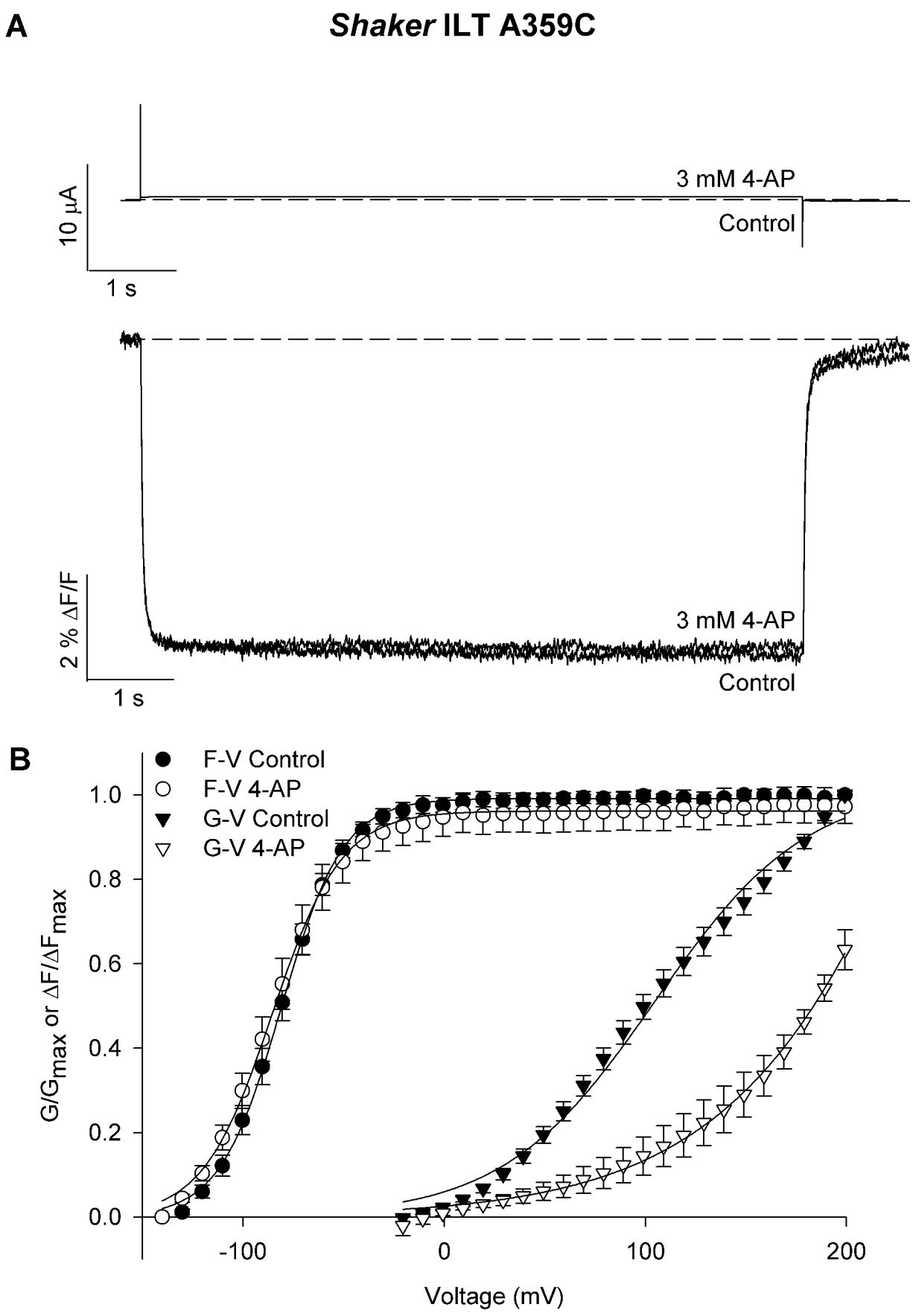

Figure 6